1

HISTORICAL PERSPECTIVE ON NANOPARTICLES IN IMAGING FROM 1895 TO 2000

Mikhail Y. Berezin

Department of Radiology, Washington University School of Medicine, St. Louis, MO, USA

1.1 INTRODUCTION

Out of the two main subjects covered in this book—imaging and technology—imaging, or more commonly referred to as radiology, "the eye of medicine," is certainly the oldest. Prior to the appearance of nanoscience, radiology had already been well established through several generations of physicians who themselves processed thousands of images every year. Still, the persistent quest to "see the invisible" to better diagnose patients forced radiologists to pay close attention to the research and development of new imaging technologies. In the past two decades, nanoparticle contrast agents, stemming from the earliest contrast agents discovered soon after the discovery of X-rays over a hundred years ago, have become the holy grail of imaging. Today, an impressive number of radiological procedures that routinely utilize nanoparticles in clinics with even more impressive number are under preclinical testing and medical research.

The National Institutes of Health (NIH) in 2002 prioritized the most pressing problems facing medical science and identified three key areas in need of research: biological pathways, molecular imaging, and nanotechnology. The focus on these three critical components, backed by substantial investments from the NIH, transformed classic radiology and early disorchestrated attempts with nanoparticles

Nanotechnology for Biomedical Imaging and Diagnostics: From Nanoparticle Design to Clinical Applications, First Edition. Edited by Mikhail Y. Berezin.

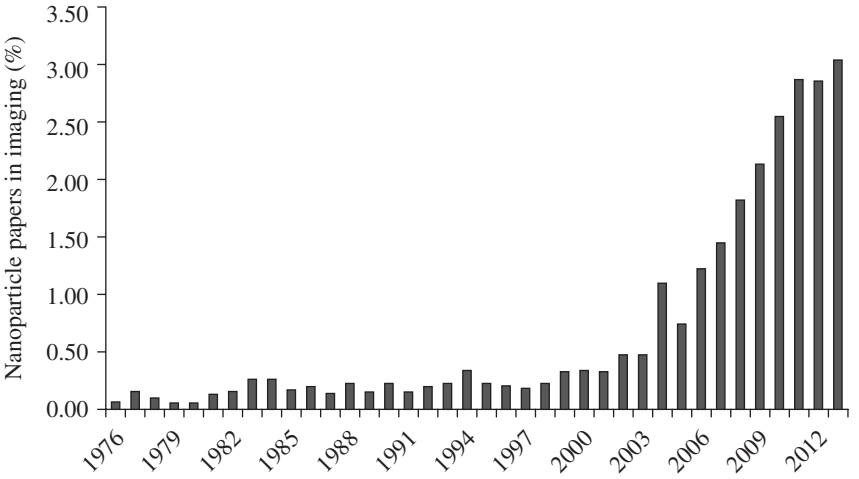

FIGURE 1.1 Growth of the nanoparticle research in biomedical imaging. Solid arrows show the appearance of imaging techniques, and dotted arrows show the emergence of nanoparticles. A number of citations are given from PubMed database.

into a mature field known today as molecular imaging. Figure 1.1 reflects a remarkable tenfold increase in nanoparticle-related medical imaging research from a relatively modest approximately 0.25–0.3% in the twentieth century to the current 3%. This growth resulted in more than 1500 nanoparticle imaging-related publications in 2012 alone.

From the onset of radiology and the first contrast agents to the end of the twentieth century, imaging techniques such as X-ray, PET, SPECT, ultrasound, MRI, optical, and photoacoustics have emerged. The first imaging nanoparticles appeared only in the middle of the twentieth century. The progress and the application of imaging nanoparticles followed the advent of new imaging modalities and diverged into two equally important directions. In one direction, de novo nanoparticle designs were developed for specific imaging modalities. Some examples include magnetic particles for MRI, quantum dots (QDs) for optical, and nanobubbles for ultrasound. The other direction adopted previously established designs of nanoparticles (for instance, for drug delivery) and modified them for imaging applications. Some examples include liposomes, virions, cross-linked nanoparticles, and surface modification to increase the nanoparticles' imaging specificity. Regardless of direction, many nanoparticles applications often began as unexpected discoveries. Many steps to refine their design were necessary to turn them from a mere curiosity to a clinically acceptable tool. Today, the continued improvement in nanoparticle synthesis, conjugation technique, and novel biomarkers made the nanoparticle approach a unique and well-differentiated scientific direction that blends seamlessly with clinical imaging. The historical trend illustrated in Figure 1.2 highlights the most important milestones toward this direction and is discussed in this chapter.

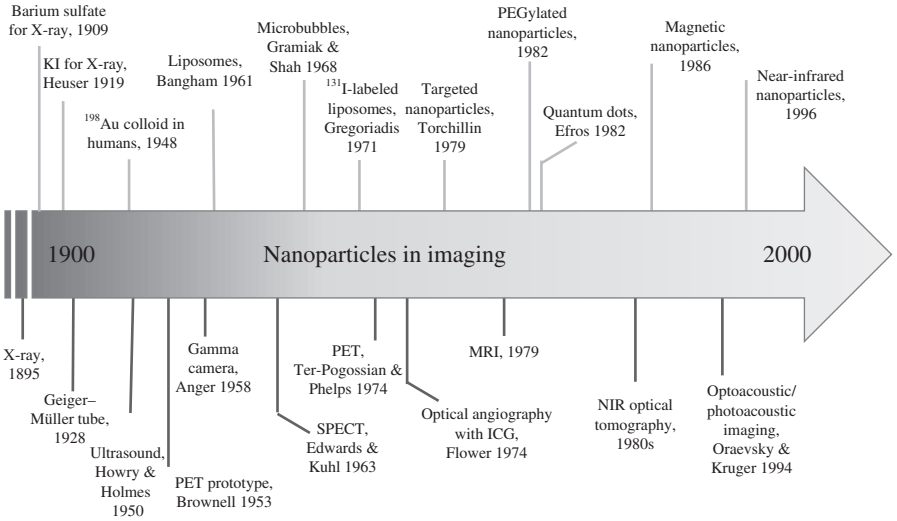

FIGURE 1.2 Timeline of the most important events in the development of nanoparticles for imaging and diagnostics covering the period from the twentieth century. The upper part corresponds to nanoparticles, and the lower part to the development of imaging modalities. (*See insert for color representation of the figure*.)

1.2 X-RAY AND FIRST CONTRAST AGENTS (1895–1930s)

The history of medical imaging started on November 8, 1895, when a 50-year-old Wilhelm Conrad Röntgen—a physicist from the University of Würzburg in Germany—observed a greenish glow from a recently invented Crookes tube. A new form of radiation, which Röntgen called an "X-ray," freely penetrated through biological tissue but was absorbed by dense material such as bones. Recorded on radiation-sensitive photographic plates, a well-recognized X-ray image was made. This entirely noninvasive imaging technique quickly spread across the world after its demonstration to the public in 1896. A review of major medical colleges across the United States conducted by the *American X-Ray Journal* (Fig. 1.3 shows the cover of this journal) in 1899 revealed more than 80 institutions where X-ray machines were available for patients [1], a remarkable rate given that it was just 4 years after X-ray discovery. With X-ray imaging, bone fractures, kidney stones, and metallic objects such as bullets and needles could be reliably located. With further refinement, physicians could even recognize and visualize certain organs. However, imaging inside the organs was impossible since the low and uniform density of soft tissue composed of transparent to X-rays water and organic media provided little contrast within the tissue.

To address this shortcoming, W. Cannon from Harvard Medical School began developing "contrast agents," biocompatible compounds that could absorb X-rays. In 1905, he discovered that high-density metal salts such as bismuth-based compounds provided the desired contrast in the intestines: "The animals thus fed with food mixed with bismuth subnitrate were exposed to the X-rays and, without disturbing the

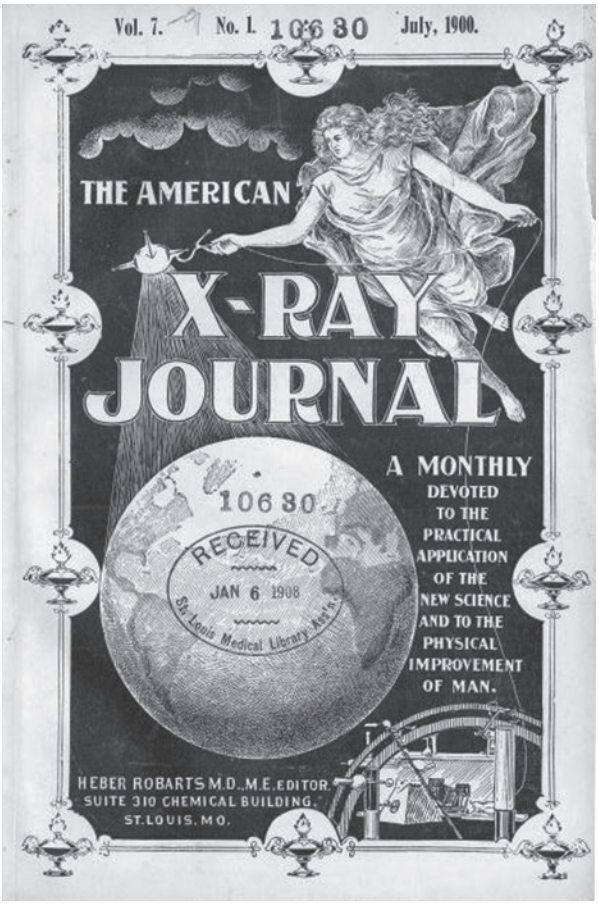

FIGURE 1.3 The *American X-Ray Journal* established in May 1897 was one of the first imaging journals. Launched by Dr. H. Robarts, a prominent radiologist from St. Louis, his biography is described in Ref. [2]. The journal existed until 1905. (Courtesy of Becker Library, Washington University School of Medicine.)

processes of digestion, the movements of the food in the stomach and small intestine were observed by means of the shadows cast on a fluorescent screen" [3]. A few years later, a less toxic barium sulfate mixed with foodstuffs became the first broadly used contrast agent in X-ray imaging of the digestive tract [4]. This water-insoluble salt (to prevent barium toxicity) was swallowed with food prior to the imaging procedure to outline the esophagus, stomach, and small intestines. The contrast could also be inserted via enemas to visualize the colon. This practice allowed the visualization of tumors, strictures, blockages, and ulcers and has been so simple and successful that it is still in use today.

The next advancement in the development of contrast agents came from Argentina, where in 1919 the radiologist Dr. C. Heuser intravenously injected a water-soluble

potassium iodide to image the circulatory system. High-density iodide provided significant attenuation to X-ray radiation, causing the blood vessels to appear lighter on film. A few years later, Heuser utilized another iodinated compound called Lipiodol synthesized in 1901 by the French chemist M. Guerbet. Lipiodol is a low-viscosity radio-opaque diagnostic agent formed by the iodination of the fatty acids in poppy-seed oil and was applied to investigate the uterine cavity and fallopian tubes. Due to its high density and low toxicity, many iodinated compounds are commonly used today in X-ray and computer tomography (CT) imaging—a successor of the X-ray technique. (One of the leading companies of X-ray contrast agents is the Guerbet Group established by the son of Lipiodol's inventor in 1926.) However, despite several decades of continuous efforts to improve X-ray instrumentation and expand X-ray imaging to soft tissue with contrast agents, diagnosing diseases of internal organs suffered from unacceptably low contrast. New technologies were desperately needed.

1.3 RISE OF THE NUCLEAR IMAGING TECHNIQUES (1940s–1950s)

Shortly after World War II in 1946, the U.S. Congress passed the Atomic Energy Act that transferred nuclear weapon development and nuclear power management to civilian, rather than military control. The Oak Ridge Laboratory in Tennessee was directed to provide radioisotopes for peaceful purposes, especially for medical applications. One of the first isotopes made available was ^{198}Au colloid. It was produced by bombarding gold foil with slow neutrons in a uranium pile and was immediately (1947) utilized for cancer therapy in patients [5]. Since gold cations are extremely reactive due to their high reduction potential ($Au^{3+}(aq) + 3e^- \rightarrow Au(s)$, +1.50 V vs. NHE), they are incompatible with biological tissues. In contrast, gold colloid is chemically stable for storage, and the author recalls seeing bottles of colloidal gold that were several decades old. In addition, gold colloid is biologically inert and has been known in medicine since the time of Paracelsus [6].

^{198}Au emits radiation consisting of 0.97 MeV beta (β^-)- and 0.411 MeV gamma (γ)-rays with a half-life of 2.7 days [7]. The beta radiation from this isotope is absorbed under several millimeters of tissue rendering its importance for cancer treatment. The gamma emission that penetrated freely through the body became important for imaging. Produced colloidal gold nanoparticles were small enough (3–7 nm) [8] to pass through the pulmonary capillaries (<7 μm) but were accumulating mostly in the liver and spleen [9]. At higher dosages, even bone marrow could be visualized. The problem with ^{198}Au was its high radiation dosage of 50–100 rad/μCi that limited its clinical utility. In the search for compounds offering better imaging properties, ^{99m}Tc–sulfur colloid has been explored. Subsequently, other radioactive colloids such as ^{68}Ga ferric oxide and ^{113}In ferric hydroxide have been employed. With the help of these nanoparticles, untreated leukemia with grossly expanded marrow compartments was shown to be distinguished from aplastic anemia or myelofibrosis with less than normal activity of marrow [10].

Following the acceptance of isotopes in imaging, the 1940s and 1950s witnessed a rapid development of imaging instrumentation. The diagnostics with radioactive metals

were generally conducted by "external counting" or "scintillation scanning." For that, a handheld Geiger–Muller counter introduced in 1928 capable of measuring gamma-rays and its mica-window modification for simultaneous detection of energetic beta-rays from *in vivo* sources was utilized [11]. By applying a Geiger–Muller counter to the surface of the skin at the site of interest, the distribution of the isotopes in the blood and extracellular tissue fluids could be followed. This method was a widely accepted standard in clinics until in 1958 when H. Anger from Berkeley Lab described a new scintillation camera (Anger camera), where gamma-rays were detected by a scintillating crystal. Upon contact with a gamma photon, a scintillator such as NaI crystal emits a photon at much lower energy, approximately 430 nm, thus converting ionizing radiation into light energy that could be detected by a photomultiplier tube (PMT). With many of the PMT tubes attached to the same crystal, many points could be imaged simultaneously. One of the first applications of the Anger camera was in a knee injected with ^{198}Au to diagnose an acute knee diffusion [12], a pathology that describes an excessive amount of fluid that accumulates around the joint and causes swelling.

Positron emission tomography (PET) and single-photon emission computed tomography (SPECT) have made their appearance in the 1950s. At the beginning of this decade, a team from MIT led by G. Brownell and physician W. Sweet from Massachusetts General Hospital [13] and independently F. Wrenn *et al*. [14] constructed the first PET detector to exploit the positron–electron annihilation effect for use as an imaging tool. D. Kuhl at the University of Pennsylvania and his colleagues at the University of Pennsylvania built the Mark II scanner, an ancestor of today's CT and SPECT scanners. The historical reviews on the development of imaging techniques written by the pioneers of this field describe these early efforts in great detail [15–17]. One of the first human scanners Mark III is shown in Figure 1.4.

Although the period of the 1940s–1950s has demonstrated the potential of imaging with nanoparticles in diagnostics and treatment monitoring, the use of nanoparticles was accidental. The majority of the efforts were directed toward the discovery of less expensive and more available sources of radioisotopes (cyclotrons, nuclear reactors), the development of imaging instrumentation, and the medical assessment of the techniques. Nanoparticles were produced mostly in the form of colloids, their chemistry has more or less been established, and their formulations were straightforward. Minimum efforts have been made to modify the nanoparticles for specific medical applications. These efforts started and went into full swing throughout the next decades.

1.4 IMAGING WITH LIPOSOMES (1960s–1970s)

1.4.1 Discovery of Liposomes

In the beginning of the 1960s, A. Bangham and his colleagues from the University of Cambridge (London) visualized the dispersion of lecithin-type phospholipids under an electron microscope and discovered their unusual multilamellar architecture (Fig. 1.5). "Toward the end of 1962, we had persuaded ourselves that we were seeing minute sacs of approximately 50 nm diameter, the first 'lipid somes' as we have come to know them." Intensive studies of the liposomes led to the discovery of aqueous

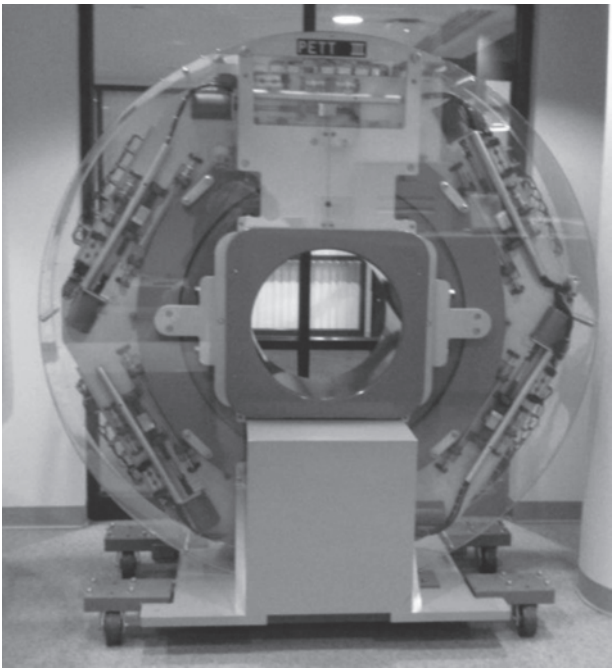

FIGURE 1.4 First human PEN scanner PETT III (1974) located in the hall of the Department of Radiology Washington University School of Medicine in St. Louis, where this scanner had been invented. The inventors had given the name "positron emission transaxial tomography" (PETT). The name was reduced to PET because transaxial was no longer the only plane used for image reconstruction. (*See insert for color representation of the figure.*)

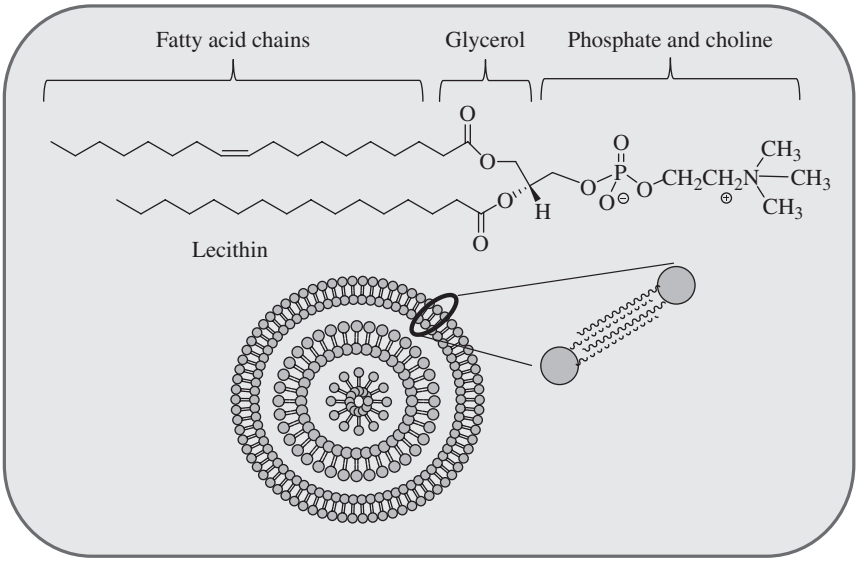

FIGURE 1.5 Structure of a multilamellar liposome and of a typical lecithin component phosphatidylcholine. The latter is composed from choline and phosphate group, glycerol, and long-chain fatty acid. Lecithin was first isolated in 1846 by the French chemist and pharmacist Theodore Gobley.

channels between lamellar structures that could be widened by the introduction of charged molecules into previously uncharged lecithin layers [18, 19]. These multilamellar liposomes were found to capture a variety of cationic species from tiny Li^+ ions to relatively large cholines and, as soon to be shown, imaging reporters that were dissolved in the aqueous phase at the time of liposome formation.

Following the discovery and characterization of multilamellar liposomes, D. Papahadjopoulos and N. Miller in 1967 described the structure of small unilamellar vesicles (SUVs) [20, 21]. This was an important development, since SUVs could be formed with better reproducibility and could serve as a technological platform for molecular imaging.

1.4.2 Visualization of Liposomes *in Vivo*

The majority of liposome clinical applications were historically centered in drug delivery. However, the visualization of the liposome distribution *in vivo* was critical for their clinical success and was the driving force behind the labeling of the liposomes with imaging reporters. In the beginning of the 1970s, G. Gregoriadis with colleagues from the Royal Free Hospital School of Medicine in London prepared liposomes labeled with entrapped ^{131}I-labeled albumin [22, 23] (Fig. 1.6). Upon *in vivo* administration, these liposomes were primarily deposited into the liver (major)

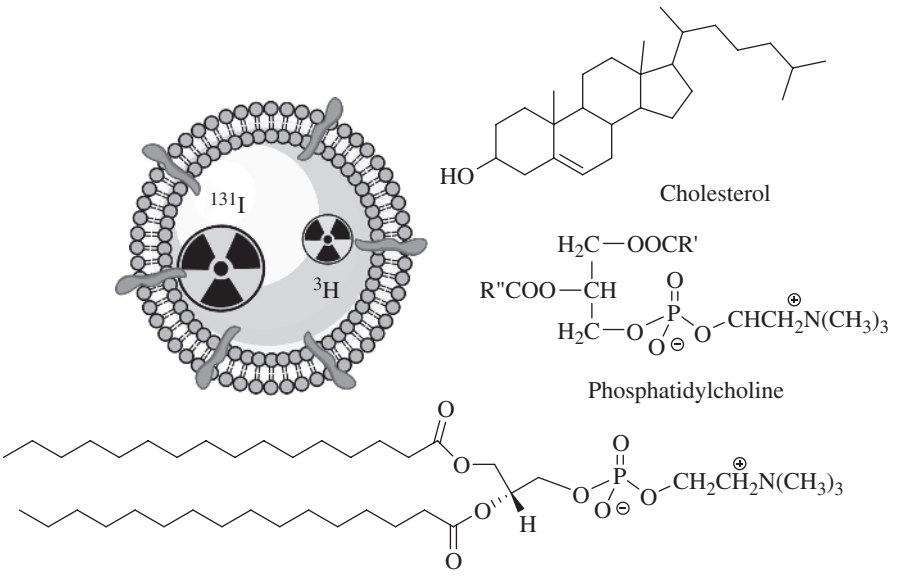

FIGURE 1.6 Design of ^{131}I-albumin liposomes. [^3H]Amyloglucosidase and ^{131}I-labeled albumin were entrapped into liposomes composed of phosphatidyl choline, cholesterol, and dicetyl phosphate. ^{131}I-labeled albumin was also entrapped in [^3H]cholesterol liposomes. (Based on Refs. [22] and [23].)

and spleen (minor), targeting Kupffer cells as well as parenchymal cells. A few years later (1974), this contrast agent was applied to cancer patients [24] to monitor the deposition of a liposome carrying radiopharmaceutical to the area of treatment. It was, in fact, the first time liposomes were administered into humans.

Realizing the potential of radiolabeled liposomes in imaging, groups of V. Caride from Yale and V. Richardson from University of London in the middle of 1970s developed a ^{99m}Tc-labeled liposome for tumor detection [25, 26]. By that time, the medical community recognized ^{99m}Tc as an excellent radioisotope for diagnostics because of its short half-life of approximately 6 h allowing for the complete clearance of radioactivity after 24 h and, also, readily detectable 140 keV γ-rays by conventional X-ray diagnostic equipment. ^{99m}Tc labels were attached to a variety of preformed liposomes made from phosphatidylcholine and cholesterol via a so-called tin chloride method shown in Figure 1.7. This method allowed ^{99m}Tc originally generated in the form of highly hydrophilic pertechnetate anion TcO_4^-, to be reduced into more hydrophobic Tc^{3+} compound and be integrated into organic environments. Upon administration of this radiolabeled liposome to mice, a significant increase of the clearance rate of radioactivity was achieved compared to free pertechnetate. More importantly, the preferential uptake of the contrast agent by tumors was observed. However, the liposomes with Tc^{3+} had low stability *in vivo* resulting in the dissociation of the radionuclide from the liposome. Hence, the tin chloride reduction method was later enhanced by the addition of ^{99m}Tc-specific chelators.

Around the same time in the 1970s, the group of J. Baldeschwieler from Stanford University came up with the visualization of liposomes from another angle. The original intention of the group was to develop a technique for monitoring the release of a therapeutic cargo from the liposomes. Certain isotopes, such as ^{111}In known well today, sequentially emit two gamma-rays of different energy. These two sequential emissions can be measured by a technique known as gamma-ray perturbed angular correlation (PAC) coincidence spectroscopy. The result of the measurement is a parameter that is related to the rotational correlation time of the label. Molecules trapped inside the liposomes rotate faster than the released ones and bound by high-molecular-weight serum proteins. Hence, the change of the environment affects (perturbs) the angular correlation and alters its rotational time. In the series of publications from 1972 to 1980, the group refined this technique, synthesized a variety of ^{111}In carrying liposomes, measured the liposomes' structural integrity *in vivo*, and

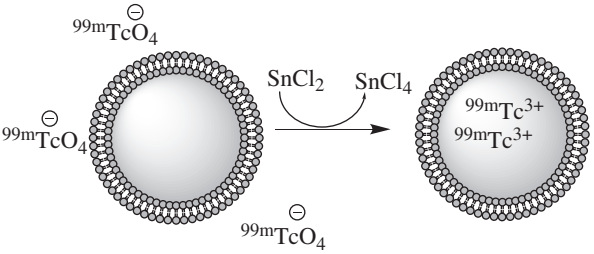

FIGURE 1.7 Formation of ^{99m}Tc liposomes via tin chloride method. (Based on Ref. [25].)

finally demonstrated tissue specificity for targeting liposomes [27–29]. One of the outcomes of this study was the recognition and the rise of a variety of ^{111}In-labeled nanoparticles for SPECT imaging [30–33].

1.5 MAGNETIC IMAGING WITH NANOPARTICLES (1980s–2000)

1.5.1 MRI Nanoparticles with Paramagnetic Ions

Clinical applications of MRI in the beginning of the 1980s, initiated by the first commercially available MRI scanners from General Electric, opened a new era in imaging. The fascinating early history of MRI contrast agents has been well documented, and the reader is encouraged to review the Reference [34]. In MRI, a strong magnetic field pulse is applied to a body causing certain atoms, such as protons, to be excited. The rate of the following relaxation is recorded and transferred into an image. This concept of relaxation came from nuclear magnetic resonance (NMR), the predecessor of today's MRI, as a method for characterizing organic compounds. By the middle of the 1970s, chemists recognized that beside three major NMR parameters, chemical shifts, coupling constants, and integrated areas, there were two more parameters, namely, spin relaxation time (T_1) and lattice relaxation time (T_2), that could be used to characterize the structure of the organic molecule [35]. Hence, there were also a number of ways whereby spin–lattice relaxation times could be chemically manipulated. Among them was the use of paramagnetic metal ions including gadolinium (Gd) that affected the relaxation times of associated ligands and nearby solvent molecules. Not surprisingly, the first MRI contrast agents described in the early 1980s were based on Gd complexes.

To enhance the MR signal, metal atoms should be freely exposed to biological water. This requirement demands the location of the metal at the exterior of the nanoparticle. To address this problem, G. Kabalka from the University of Tennessee in 1987 prepared Gd complexes with DTPA carrying two lipophilic long chains that were integrated into the lamellar phase of liposome particles [36] (Fig. 1.8). This proof-of-concept approach showed that the relaxation rate in the liver, post *ex vivo*, increased by 180%. Other metal complexes such as Mn^{2+} complexes have been also explored. The early attempts to entrap Mn^{2+}-DTPA in multilamellar liposomes [37] were not entirely successful; the complex from nanoparticles leaked out although the image showed the difference in contrast agent biodistribution compared to the free complex. In a parallel effort, the group of G. Navon from Tel-Aviv University added serum albumin to stabilize the complex inside the liposome and enhance their effect on water proton relaxation rates [38]. However, these promising *in vitro* results were not followed by imaging *in vivo*.

1.5.2 Supermagnetic Nanoparticles

The breakthrough in the development of MRI contrast agents began from the introduction of supermagnetic nanoparticles in the mid-1980s. In contrast to by that time popular T_1 Gd paramagnetic agents, this class of contrast agents gave rise to a dramatic

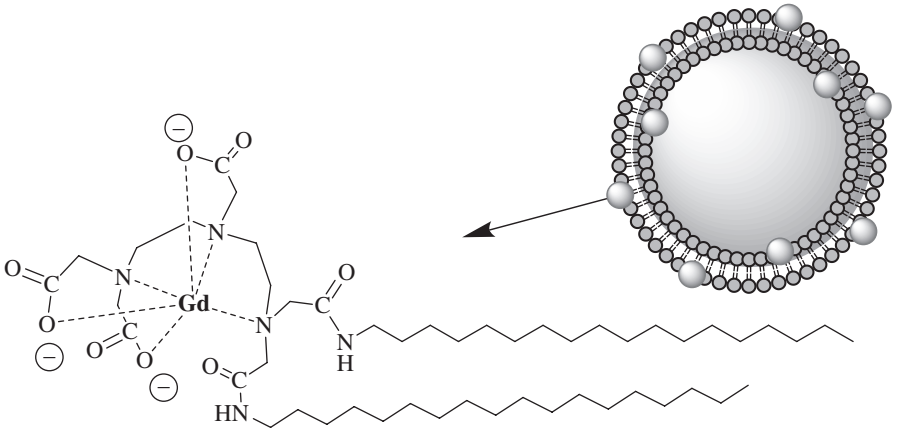

FIGURE 1.8 Amphipathic Gd complex with DTPA featuring hydrophobic tails. DTPA anhydride was reacted with stearyl amines and integrated into the lamellar phase of liposome particles. The T_1 in the liver increased by 180%. (Based on Ref. [36].)

shortening of the T_2 or T_2* relaxation times. A group led by J. Leigh Jr., a radiology scientist at the University of Pennsylvania, introduced ferromagnetic, albumin-coated magnetite particles of 1–50 nm in diameter [39]. These nanoparticles, prepared from ferric and ferrous chlorides, were covered with cross-linked albumin to decrease potential metal toxicity and showed significant reduction of both T_1 and T_2 at relatively low particle concentration in rats. At the same time, P. Lauterbur's group from the State University of New York, Stony Brook, reported enhanced imaging of the abdomen in dogs using 50 nm magnetite nanoparticles [40]. (The contribution of P. Lauterbur in MRI was acknowledged with a Nobel Prize in 2003.) Both Leigh's and Lauterbur's groups predicted the success of ferromagnetic nanoparticles in future biomedical research and clinical diagnosis.

In the upcoming years, the potential of many types and sizes of superparamagnetic particles (SMP), micrometer-sized paramagnetic iron oxide (MPIO, micron size), superparamagnetic iron oxide (SPIO, submicron size), and ultrasmall superparamagnetic iron oxide (USPIO, <50 nm) has been evaluated in many preclinical and clinical trials. The acceptance of these particles in research and clinical applications was mainly due to the following advantages: (i) a strong change in the signal per iron atom, in particular on T_2-weighted images (given thousands of iron atoms in the nanoparticle, the strength of the signal overcomes the typical low contrast agent sensitivity of MRI); (ii) the biocompatibility of relatively low toxicity iron—free iron can be metabolized via normal biochemical pathways; and (iii) coating and surface modifications, allowing the active targeting of the nanoparticles [41]. Many of the SMP nanoparticles have been commercialized and approved by healthcare systems in Europe and Asia under the trade names of Endorem®, Guerbet SA, or Ferridex®, Berlex Laboratories, Inc. By the turn of the twenty-first century, contrast agents were used in nearly 25% of all MRI procedures.

1.6 OPTICAL IMAGING WITH NANOPARTICLES (1980s–2000)

Optical imaging was one of the newest imaging modalities that marked its debut for deep tissue imaging less than two decades ago. Although observation of visually accessible body parts and some organs (such as the colon, throat) has been accessed for centuries, the use of light to visualize internal organs did not begin until the mid-1970s. Diaphanography [42] (a method for the evaluation of the female breast) and eye angiography (see Section 1.6.1 "NIR cyanine dyes") were one of the first clinical applications of imaging with light in the 1970s. Typical visible photons do not penetrate through biological tissues deeper than several millimeters due to extensive scattering of photons by the tissue and significant levels of endogenous chromophores such as melanin and hemoglobin that absorb visible photons. In contrast, near-infrared (NIR) light (700–900 nm) can penetrate the tissue much deeper: the scattering is lower and the endogenous absorption in this spectral range is weak. With the development of NIR instrumentation such as detectors, light sources, and especially NIR contrast agents in the middle of the 1990s, optical imaging quickly advanced from a preclinical stage to use in clinical applications.

1.6.1 NIR Cyanine Dyes

A large number of today's nanoparticle research involves decorating nanoparticles with fluorescent NIR dyes from a class of cyanines. The history of cyanine dyes for imaging applications started in the middle of the 1950s when an executive of Eastman Kodak Company, who was pleased with the care he received from Dr. I. Fox at the Mayo Clinic, offered to help him in his research. Dr. Fox needed a biocompatible dye that could be detected in blood. The executive sent an array of dyes from the Eastman Kodak laboratories for evaluation. Included among them was indocyanine green (ICG) (Fig. 1.9) developed as a sensitizer for photography by D. Heseltine and L. Brooker [43]. The testing for measuring hepatic function began in 1957 [44], and due to the low toxicity, the compound was rapidly approved by the FDA for this application in the beginning of 1959. Several years later, this dye was clinically used for measuring cardio function from ICG blood clearance curves.

The first attempt at using ICG for angiography was conducted by K. Kogure and coworkers from the University of Miami in 1968 when they demonstrated

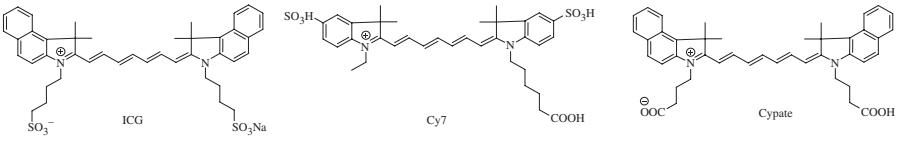

FIGURE 1.9 Structures of NIR dyes: indocyanine green, first approved near-infrared dye developed by Kodak chemists Heseltine and Brooker in 1957 [44], Cy7 developed by Waggoner (1987) and later commercialized by Amersham [47, 48], and cypate (2000) synthesized by Achilefu [49].

infrared absorption angiography of a monkey's brain vasculature [45]. Following intra-arterial ICG injection, the brain was illuminated by a flash from a bright lamp, and images were recorded on a Kodak Ektachrome film with sensitivity up to 900 nm. However, the method did not work with intravenous injections. In the early 1970s, R. Flower and B. Hochheimer at Johns Hopkins discovered the NIR fluorescence of ICG that was especially strong in blood samples and that could be visualized with night vision scopes or sensitive NIR films. In 1972, the first intravenously injected ICG fluorescence angiograms were produced. The early history of these events and their following development are described in References 43 and 46.

Following its success in ophthalmology, ICG was exploited in cancer diagnostics in 1994 to delineate tumor margins [50]. To overcome the disadvantage of fast clearance (half-life is 3.4 min in humans) and for better confinement in blood vessels, Devoisselle with colleagues prepared ICG incorporated in liposomes [51]. Expectedly, a substantially longer residence time (>60 min) was achieved when administered to rodents compared to the free dye.

The use of ICG was restricted to mostly simple formulations or direct injections of the dye. Lack of active functionalities precluded the use of ICG for labeling. A. Waggoner from Carnegie Mellon University addressed this problem by developing a set of cyanine dyes including NIR dye Cy7 with reactive functionalities such as NHS esters and isothiocyanate [47, 48]. Cy7 commercialized by Amersham (now GE Healthcare) became one of the most utilized NIR dyes in the 1990s. In parallel, S. Achilefu (then at Mallinckrodt, Inc.) developed cypate, an activatable analog of ICG, with almost identical optical properties to ICG (molar absorptivity, quantum yield) [49]. Other reactive NIR dyes followed [52], and the imaging using the dyes of conjugated to antibodies and small peptides has been demonstrated *in vivo* in mouse models [53]. These functionalizable NIR dyes have later become the dyes of choice for labeling many types of nanoparticles.

1.6.2 QDs

The term "quantum dots" was coined by Mark Reed (then at Texas Instruments) in his paper published in 1988 [54]. The introduction of QDs started with the realization that the optical properties of semiconductor particles were strongly dependent on particle size due to the quantum confinement of the charge carriers in small spaces. Thus, at a certain small size, the semiconductors could turn into bright emitters. A theoretical framework for these size-dependent properties was first described by brothers Alexander and Aleksei Efros from Ioffe Institute in the USSR in 1982 [55]. Shortly after their publication, publications describing synthesis of QDs emerged from several researchers. Among them, L. Brus (from Bell Labs) was awarded with the first Kavli Prize in Nanoscience in 2008 for his pioneering efforts in this field [56]. (The prize was actually shared with Sumio Iijima, of Meijo University in Japan, for his discovery of carbon nanotubes—another prominent imaging agent—of which its potential in imaging became recognized in the 2000s.)

For almost a decade, QDs with their low quantum yield and instability remained a subject of interest chiefly among physicists and material scientists. Three steps toward

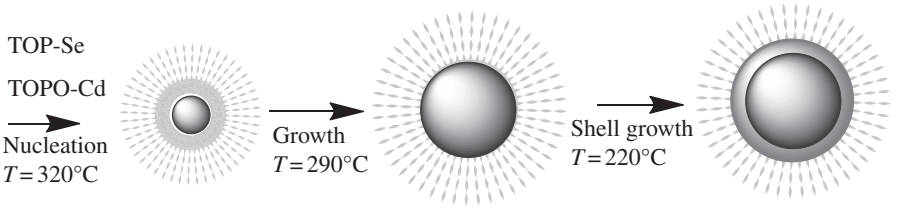

FIGURE 1.10 High-temperature synthesis of colloidal CdSe quantum dots. A Cd precursor is dissolved in the tri-n-octylphosphine oxide (TOPO)-coordinating solvent. Under continuous stirring at high temperature (~320°C), a Se precursor dissolved in tri-n-octylphosphine (TOP) is injected into the flask, initiating nucleation of CdSe nanoparticles. The growth phase occurs at lower temperature (to ~290°C). When the desired size has been obtained, the solution is cooled (~220°C) to prevent further particle growth. A passivating layer of ZnS is deposited by injection of zinc and sulfur precursors dissolved in TOP. Upon cooling to room temperature, these core–shell QDs are isolated via precipitation. (Based on Ref. [57].)

bioimaging applications have been made in following years. The first step was to increase the brightness and stability of QDs with a protective layer. The synthesis of such protected CdSe/ZnS QTs with tunable emission was developed by the M. Bawendi group [57] and is shown in Figure 1.10. The produced QDs were highly fluorescent but only soluble in organic solvents such as toluene. Hence, another critical step toward biomedical applications was making the QDs hydrophilic. In 1998, two groups led by P. Alivisatos at UC, Berkeley, and S. Nie at Indiana University, Bloomington, independently demonstrated that QDs could be made water soluble and could be conjugated with biological molecules [58, 59]. The final step toward *in vivo* imaging was the development of QDs emitting above 700 nm. This step was introduced only in 2004 in a joint publication from Bawendi and Frangioni [60] and is part of the new history of imaging nanoparticles.

1.6.3 Nanoparticles as Photoacoustics Contrast Agents

One of the promising applications of optical nanoparticles is their utility as contrast agents in photoacoustics. Although the effect of photoacoustics or (optoacoustics) has been demonstrated long time ago in 1880 with the pioneering work of Alexander Graham Bell, photoacoustics became an imaging modality only recently. The early works by Oraevsky *et al*. [61] and Kruger *et al*. [62] demonstrated the value of photoacoustic signal in imaging of deep tissue in the early 1990s. Several years later, prolated metal nanoparticles absorbing at 1064 nm were suggested as contrast agents by Oraevsky's group [63, 64].

1.7 ULTRASOUND MICROBUBBLE CONTRAST AGENTS (1970s–2000)

Technically, microbubbles are vehicles that exceed the size of nanoparticles with a diameter in the 1–10 μm range. However, the recent trend of minimizing their size to nanosized scales prompts us to cover microbubbles in this chapter.

Ultrasound was primarily developed for military applications for detecting submarines in World War I. In the late 1940s, several enthusiasts recognized the potential of this technique in medical imaging. Among them was a radiologist D. Howry. In his basement in Denver, Howry, later together with the nephrologist J. Holmes, built his first ultrasound scanner to image soft tissue [65]. The principle of imaging was based on the reflection of an ultrasound signal generated by a piezoelectric transducer at some fundamental frequency. This ultrasound signal travels through the biological tissue, gets reflected off a structure, and travels back to the transducer to produce an image. After a decade of development, the technique underwent significant modifications, and by the mid-1960s, the first commercial system, Vidoson® by Siemens, Inc., for ultrasound imaging was released.

However, due to poor reflection of signal against biological tissue, measured signal intensity was low, producing images of poor quality. By serendipity, Raymond Gramiak, a radiologist at the University of Rochester, while examining a patient for cardiac output with indocyanine green—a standard method at that time—observed an intense contrast improvement at the site of injection [66]. In the following paper, the authors identified a small amount of foam formed upon dissolution of ICG with water responsible for the intracardiac contrast effect produced by ICG. "It is our belief that the contrast effect represents the ultrasonic detection of miniature bubbles within the heart produced by gaseous cavitation, which occurs when the contrast agent is injected rapidly, or by miniature bubbles injected in the foam of indocyanine-green solutions [67]." This discovery paved the way to an era of numerous designs of micro- and, later, nanobubbles in the following decades that are covered in many reviews and books [68–70].

The clinical use of early contrast agents that were made on site by agitation of saline solutions filled with air were unsuccessful due to the low stability of air-filled microbubbles and rapid disappearance of the contrast signal *in vivo*. The early agents also suffered from large and heterogeneous sizes and low permeability through the pulmonary system. Subsequent efforts showed that the stability of the microbubbles could be enhanced via a sonication technique instead of agitation and could be further improved by stabilizing agents such as sorbitol and dextrose [71]. Among the new techniques, a patent filed by Feinstein in 1985 [72] introduced a new class of stabilized microbubbles. These microbubbles were formed by sonication of an albumin solution that led to the formation of a protective coating of serum albumin on the surface of the bubbles [68] (Fig. 1.11). This discovery headed to the development of the first generation of the commercial contrast agent Albunex® (Mallinckrodt, Inc.) with a thin layer of cross-linked albumin (<15 nm) around an air bubble. The advantage of this contrast agent was that Albunex could be purchased in a standardized prepackaged form, minimizing handling complications and errors with dosage.

Despite the presence of protective layers, the microbubbles were still suffering from short lifetimes in circulation. Due to their relatively large size, they were unable to cross the lung barrier, thus limiting the imaging to the right side of the heart. Addressing these problems, the second-generation contrast agents were filled with a heavy gas such as perfluoropropane. The use of the high-density gas as a filling material was a breakthrough since it drastically reduced the diffusion of the gas from

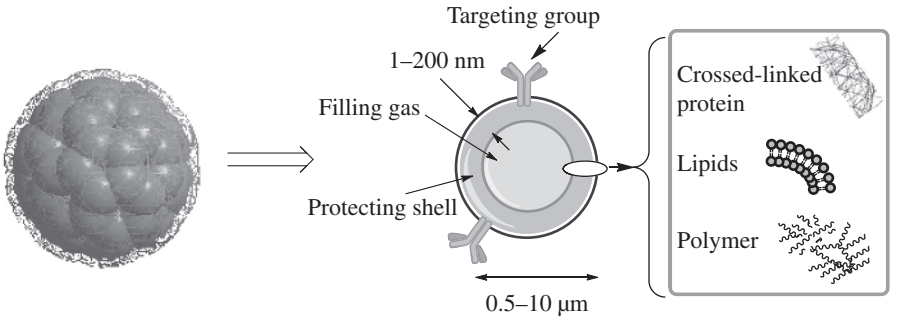

FIGURE 1.11 Schematic of a microbubble with a protecting shell and targeting groups. (Based on Ref. [68].)

the bubble due to the low solubility of perfluorinated molecules in the blood. The high stability of the microbubbles allowed imaging at much lower dosages and with longer imaging time. In addition, these new-generation microbubbles such as Optison (Mallinckrodt, Inc.) were approved by the FDA in 1997 and were much smaller with diameters less than 4 μm, allowing for the imaging of the whole heart.

1.8 MATURITY: NANOPARTICLES SURFACE MODIFICATIONS (LATE 1980s–EARLY 2000s)

By the middle of 1980s, several imaging techniques became suitable for the identification of internal organ pathologies. The ability to perform diagnostics noninvasively had a profound effect on the practice of medicine. New contrast agents became commercialized and rapidly adopted by clinics, which further accelerated the search for new contrast agents including nanoparticles. However, the available methods and contrast agents to highlight pathological changes could not be utilized for early diagnostics, where the change in signal was often below the resolution of the instrumentation. Furthermore, practically all types of nanoparticles were removed rapidly from circulation by phagocytic cells of the reticuloendothelial system (RES). As a result, nanoparticles mostly resided in the liver and the spleen. The effect of the RES could have been hypothetically evaded by using large doses of nanoparticles or pharmacological interventions to inactivate macrophages, but such strategies could compromise the immune system of patients [73]. Thus, a realization emerged that nanoparticles should be modified to alter their clearance pathway and directed (targeted) to specific tissues.

1.8.1 Targeting of Nanoparticles

By the middle of the 1970s, liposomes have been the most advanced type of nanoparticles and presented an excellent scaffold for the incorporation of different types of molecules including multiple targeting moieties from small molecules to antibodies.

Multiple ligands were sought to provide additional benefits increasing the specificity of the probe due to many interactions with cell receptors overexpressed at the site of interest. The first effort to modify the surface of the nanoparticles with antibodies appeared in the mid-1970s with the pioneering work of Gregoriadis. He demonstrated that ^{111}In-labeled liposomes carrying "homing probes" such as IgG and desialylated fetuin improved the selectivity of internalization in cell studies [33]. Further progress was made by V. Torchillin's group that decorated liposomes with covalently conjugated anticanine cardiac myosin antibodies. These targeted liposomes carrying ^{111}In radiolabels, named "immunoliposomes," were administered to dogs and were shown to localize in acute canine myocardial infarctions, thus providing one of the first examples of target imaging *in vivo* [42]. In addition to antibodies, the surfaces of the nanoparticles were also modified with carbohydrates. Exposed 6-aminomannose moieties, through covalent attachments to cholesterol imbedded in the lipid bilayers (see Fig. 1.12), produced a dramatic change in the biodistribution of nanoparticles labeled with radiolabels and significantly reduced the uptake by the RES [74].

Following liposomes, the development of targeted microbubbles was initiated during the late 1990s by F. Villanueva *et al*. from the University of Pittsburgh. A 40-fold increase in the extent of monoclonal antibody-labeled bubble adhesions to activated coronary artery endothelium cells compared to nontargeted contrast agents was observed [75].

Similar to other nanoparticles of that time, early magnetite nanoparticles as a result of RES sequestration were mostly utilized for imaging of the liver, spleen, and bone narrow system. Because of RES, these nanoparticles also suffered a short blood lifetime. Hence, a significant effort over the following several years had been made to develop new synthetic routes and surface modification techniques to increase the lifetime and alter biodistribution and pharmacokinetics of iron oxide nanoparticles [41, 76].

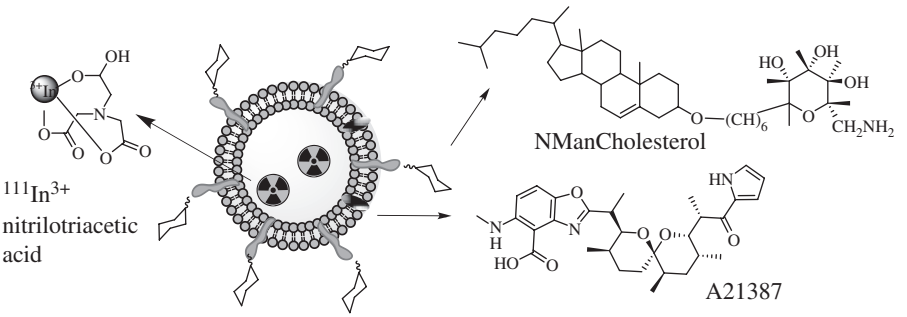

FIGURE 1.12 Design of targeted liposomes: cholesterol acts as a carrier for the targeting group, ^{111}In is complexed by nitrilotriacetic acid, and A21387 acts as a cation ionophore, allowing these ions to cross cell membranes. The key modification was a sugar derivative of cholesterol, a standard building block that adds fluidity to the liposome. The presence of particular surface carbohydrate modifications affected dramatically the stability and tissue specificity in mice. (Based on Ref. [74].)

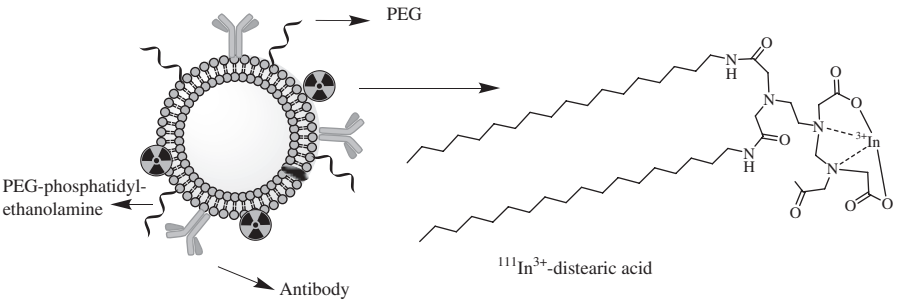

FIGURE 1.13 Immunoliposomes labeled with ^{111}In-EDTA-SA complex incorporated into the lipidic bilayer were modified with a PEG5000 derivative of phosphatidylethanolamine in combination with a monoclonal antibody to target myosin heavy chain. (Based on Ref. [79].)

1.8.2 PEGylation of Nanoparticles

Besides targeting, another important development in nanoparticle design was the introduction of polyethylene glycol (PEG). This inert hydrophilic polymer was introduced around 1970 by F. Davis, at Rutgers University, to modify bioactive proteins for medical applications to extend blood life and control immunogenicity of the proteins [77]. In 1988, A. Gabizon and D. Papahadjopoulos published a seminal paper describing a concept of PEGylated liposomes with increased retention time [78]. In this publication, a shell of PEG of up to 5–10 kDa around liposomes largely prevented the uptake by RES rendering liposomes more accessible to other organs including implanted tumors. The potential of the PEGylated nanoparticles in imaging was further revealed in 1991 by a publication from Torchillin's group [79]. In this report, liposomes labeled with ^{111}In complex were modified with a PEG5000 derivative of phosphatidylethanolamine (Fig. 1.13). Because of the presence of PEG, the liposomes cleared slowly from the blood after intravenous injection and showed up to 6–18-fold at the specific localization of the target.

1.9 CONCLUDING REMARKS

By the beginning of the twenty-first century, many diagnostic modalities, including PET, SPECT, CT, MRI, optical angiography, and ultrasound, became routine clinical tools. Emerging modalities such as optical tomography, photoacoustics, and Raman and fluorescence imaging have also begun their way into clinics. Hardware development, novel and faster algorithms, sophisticated image acquisition, and better processing software to further improve the resolution and accelerate the diagnostic procedures also emerged. After several decades of research, facing problems such as batch-to-batch variation, low *in vivo* stability, liver clogging, and legal issues that required testing of each nanoparticle component, large clinical trials with nanoparticles have finally been completed. Many imaging agents were approved by the FDA and other regulatory agencies abroad. The advances in chemistry, material science,

and analytical chemistry along with progress in molecular and cell biology, genome decoding, and the unraveling of the molecular pathways with the discovery of many disease-specific biomarkers gave rise to a new generation of high affinity contrast agents. These targeted agents increasingly in a form of nanoparticles opened up a new and exciting field of *molecular imaging*. This concept defined by R. Weisleder in 2001 as "*in vivo* characterization and measurement of biologic processes at the cellular and molecular level" [80] in contrast to the classic imaging techniques relying on changes in gross anatomy became the guide for the development of many modern imaging modalities. Many of the new advances are further discussed in this book.

REFERENCES

[1] Robarts H, editor. *X-Ray in Medical Colleges*. Volume **5**, St. Louis, MO: American X-Ray Publishing Company; 1899. p 679–686.

[2] Brown P. American martyrs to radiology. Heber Robarts (1852–1922). 1936. Am J Roentgenol 1995;**165**:473–476.

[3] Cannon WB. The passage of different food-stuffs from the stomach and through the small intestine. Am J Physiol 1904;**12**:387–418.

[4] Cannon WB. *The Mechanical Factors of Digestion*. New York: Longmans, Green & Co.; 1911.

[5] Sheppard C, Goodell J, Hahn P. Colloidal gold containing the radioactive isotope Au-198 in the selective internal radiation therapy of diseases of the lymphoid system. J Lab Clin Med 1947;**32**:1437–1441.

[6] Dykman LA, Khlebtsov NG. Gold nanoparticles in biology and medicine: recent advances and prospects. Acta Naturae 2011;**3**:34–55.

[7] Levy PW, Greuling E. The radiations from 2.7-day Au^{198}. Phys Rev 1949;**75**:819.

[8] Wheeler HB, Jaques WE, Botsford TW. Experiences with the use of radioactive colloidal gold in the treatment of cancer. Ann Surg 1955;**141**:208.

[9] Mellgren JAN, Knutsson F, Norin T. Localization and effect of injected radioactive gold (Au198) in the treatment of malignant tumors. Acta Pathol Microbiol Scand 1954;**34**: 393–409.

[10] Wagner HN. Current research in nuclear medicine. Am J Roentgenol 1970;**109**: 668–675.

[11] Strajman E. Small mica window Geiger-Müller counter for measurements of radioactive isotopes *in vivo*. Rev Sci Instrum 1946;**17**:232–234.

[12] Mallard JR, Peachey CJ. A quantitative automatic body scanner for the localisation of radioisotopes *in vivo*. Br J Radiol 1959;**32**:652–657.

[13] Brownell GL, Sweet WH. Localization of brain tumors with positron emitters. Nucleonics 1953;**11**:40–45.

[14] Wrenn FR, Good ML, Handler P. The use of positron-emitting radioisotopes for the localization of brain tumors. Science 1951;**113**:525–527.

[15] Nutt R. The history of positron emission tomography. Mol Imaging Biol 2002;**4**:11–26.

[16] Brownell GL. A history of positron imaging. Physics Research Laboratory; October 15, 1999; Massachusetts General Hospital, MIT; 1999.

[17] Thomas A, Banerjee AK, Busch U. *Classic Papers in Modern Diagnostic Radiology*. Berlin/New York: Springer; 2005.

[18] Bangham AD, Horne RW. Negative staining of phospholipids and their structural modification by surface-active agents as observed in the electron microscope. J Mol Biol 1964;**8**:660–668.

[19] Bangham AD, Standish MM, Watkins JC. Diffusion of univalent ions across the lamellae of swollen phospholipids. J Mol Biol 1965;**13**:238–252.

[20] Papahadjopoulos D, Miller N. Phospholipid model membranes. I. Structural characteristics of hydrated liquid crystals. Biochim Biophys Acta 1967;**135**:624–638.

[21] Papahadjopoulos D, Watkins JC. Phospholipid model membranes. II. Permeability properties of hydrated liquid crystals. Biochim Biophys Acta 1967;**135**:639–652.

[22] Gregoriadis G, Ryman BE. Liposomes as carriers of enzymes or drugs: a new approach to the treatment of storage diseases. Biochem J 1971;**124**:58P.

[23] Gregoriadis G, Ryman BE. Fate of protein-containing liposomes injected into rats. Eur J Biochem 1972;**24**:485–491.

[24] Gregoriadis G, Wills EJ, Swain CP, Tavill AS. Drug-carrier potential of liposomes in cancer chemotherapy. Lancet 1974;**1**:1313–1316.

[25] Richardson VJ, Jeyasingh K, Jewkes RF, Ryman BE, Tattersall MH. Properties of [99mTc] technetium-labelled liposomes in normal and tumour-bearing rats. Biochem Soc Trans 1977;**5**:290–291.

[26] Caride VJ, Taylor W, Cramer JA, Gottschalk A. Evaluation of liposome-entrapped radioactive tracers as scanning agents. Part 1: organ distribution of liposome [99mTc-DTPA] in mice. J Nucl Med 1976;**17**:1067–1072.

[27] Hwang KJ, Mauk MR. Fate of lipid vesicles *in vivo*: a gamma-ray perturbed angular correlation study. Proc Natl Acad Sci U S A 1977;**74**:4991–4995.

[28] Mauk MR, Gamble RC. Stability of lipid vesicles in tissues of the mouse: a gamma-ray perturbed angular correlation study. Proc Natl Acad Sci U S A 1979;**76**:765–769.

[29] Meares CF, Sundberg MW, Baldeschwieler JD. Perturbed angular correlation study of a haptenic molecule. Proc Natl Acad Sci U S A 1972;**69**:3718–3722.

[30] Sundberg MW, Meares CF, Goodwin DA, Diamanti CI. Selective binding of metal ions to macromolecules using bifunctional analogs of EDTA. J Med Chem 1974;**17**:1304–1307.

[31] Grove RB, Eckelman WC, Reba RC. Distribution of labeled bleomycin in normal and tumor-bearing mice. J Nucl Med 1973;**14**:917–919.

[32] Thakur ML. The preparation of Indium-111 labelled bleomycin for tumour localisation. Int J Appl Radiat Isot 1973;**24**:357–359.

[33] Gregoriadis G, Neerunjun ED. Homing of liposomes to target cells. Biochem Biophys Res Commun 1975;**65**:537–544.

[34] de Haën C. Conception of the first magnetic resonance imaging contrast agents: a brief history. Top Magn Reson Imaging 2001;**12**:221–230.

[35] Hall LD. Tate and Lyle Lecture. Spin-lattice relaxation: a fourth dimension for proton n. m. r. spectroscopy. Chem Soc Rev 1975;**4**:401–420.

[36] Kabalka G, Buonocore E, Hubner K, Moss T, Norley N, Huang L. Gadolinium-labeled liposomes: targeted MR contrast agents for the liver and spleen. Radiology 1987;**163**:255–258.

[37] Caride VJ, Sostman HD, Winchell RJ, Gore JC. Relaxation enhancement using liposomes carrying paramagnetic species. Magn Reson Imaging 1984;**2**:107–112.

[38] Navon G, Panigel R, Valensin G. Liposomes containing paramagnetic macromolecules as MRI contrast agents. Magn Reson Med 1986;**3**:876–880.

[39] Renshaw PF, Owen CS, McLaughlin AC, Frey TG, Leigh JS. Ferromagnetic contrast agents: a new approach. Magn Reson Med 1986;**3**:217–225.

[40] Dias MHM, Lauterbur PC. Ferromagnetic particles as contrast agents for magnetic resonance imaging of liver and spleen. Magn Reson Med 1986;**3**:328–330.

[41] Tiefenauer LX, Kuehne G, Andres RY. Antibody-magnetite nanoparticles: in vitro characterization of a potential tumor-specific contrast agent for magnetic resonance imaging. Bioconjug Chem 1993;**4**:347–352.

[42] Ohlsson B, Gundersen J, Nilsson D-M. Diaphanography: a method for evaluation of the female breast. World J Surg 1980;**4**:701–705.

[43] Flower RW. Evolution of indocyanine green-dye choroidal angiography. Opt Eng 1995; **34**:727–736.

[44] Fox I, Brooker L, Heseltine D, Essex H, Wood E. A tricarbocyanine dye for continuous recording of dilution curves in whole blood independent of variations in blood oxygen saturation. Proc Staff Meet Mayo Clin 1957;**32**:478–484.

[45] Choromokos EA, David NJ, Justice J Jr. The beginnings of indocyanine green angiography. J Ophthalmic Photogr 1994;**16**:70.

[46] Yannuzzi LA, Flower RW, Slakter JS. *Indocyanine Green: Angiography*. St. Louis (MO): Mosby; 1997.

[47] Ernst LA, Gupta RK, Mujumdar RB, Waggoner AS. Cyanine dye labeling reagents for sulfhydryl groups. Cytometry 1989;**10**:3–10.

[48] DeBiasio R, Bright GR, Ernst LA, Waggoner AS, Taylor DL. Five-parameter fluorescence imaging: wound healing of living Swiss 3T3 cells. J Cell Biol 1987;**105**:1613–1622.

[49] Achilefu S, Dorshow RB, Bugaj JE, Rajagopalan R. Novel receptor-targeted fluorescent contrast agents for *in vivo* tumor imaging. Invest Radiol 2000;**35**:479–485.

[50] Haglund MM, Hochman DW, Spence AM, Berger MS. Enhanced optical imaging of rat gliomas and tumor margins. Neurosurgery 1994;**35**:930–940; discussion 940–941.

[51] Devoisselle J-M, Soulie-Begu S, Mordon SR, Mestres G, Desmettre T, Maillols H. Effect of indocyanine green formulation on blood clearance and *in vivo* fluorescence kinetic profile of skin. Proc SPIE 1995;**2627**:100–108.

[52] Becker A, Riefke B, Ebert B, Sukowski U, Rinneberg H, Semmler W, Licha K. Macromolecular contrast agents for optical imaging of tumors: comparison of indotricarbocyanine-labeled human serum albumin and transferrin. Photochem Photobiol 2000;**72**: 234–241.

[53] Mariani G, Lasku A, Balza E, Gaggero B, Motta C, Luca LD, Dorcaratto A, Viale GA, Neri D, Zardi L. Tumor targeting potential of the monoclonal antibody BC-1 against oncofetal fibronectin in nude mice bearing human tumor implants. Cancer 1997;**80**: 2378–2384.

[54] Reed MA, Randall JN, Aggarwal RJ, Matyi RJ, Moore TM, Wetsel AE. Observation of discrete electronic states in a zero-dimensional semiconductor nanostructure. Phys Rev Lett 1988;**60**:535–537.

[55] Efros AL, Efros AL. Interband absorption of light in a semiconductor sphere. Sov Phys Semicond 1982;**16**:772–775.

[56] Editorial. The many aspects of quantum dots. Nat Nanotechnol 2010;**5**:381.

[57] Murray CB, Norris DJ, Bawendi MG. Synthesis and characterization of nearly monodisperse CdE (E = sulfur, selenium, tellurium) semiconductor nanocrystallites. J Am Chem Soc 1993;**115**:8706–8715.

[58] Bruchez M, Moronne M, Gin P, Weiss S, Alivisatos AP. Semiconductor nanocrystals as fluorescent biological labels. Science 1998;**281**:2013–2016.

[59] Chan WCW, Nie SM. Quantum dot bioconjugates for ultrasensitive nonisotopic detection. Science 1998;**281**:2016–2018.

[60] Kim S, Lim YT, Soltesz EG, De Grand AM, Lee J, Nakayama A, Parker JA, Mihaljevic T, Laurence RG, Dor DM, Cohn LH, Bawendi MG, Frangioni JV. Near-infrared fluorescent type II quantum dots for sentinel lymph node mapping. Nat Biotechnol 2004;**22**:93–97.

[61] Oraevsky AA, Jacques SL, Esenaliev RO, Tittel FK. Laser-based optoacoustic imaging in biological tissues. Proc SPIE 1994;**2134**:122–128.

[62] Kruger RA, Liu P. Photoacoustic ultrasound: pulse production and detection in 0.5% Liposyn. Med Phys 1994;**21**:1179–1184.

[63] Oraevsky A, Oraevsky AN. On a plasmon resonance in ellipsoidal nanoparticles. Quantum Electron 2002;**32**:79.

[64] Oraevsky AA, Karabutov AA, Savateeva EV. Enhancement of optoacoustic tissue contrast with absorbing nanoparticles. Proc SPIE 2001;**4434**:60–69.

[65] Goldberg BB, Gramiak R, Freimanis AK. Early history of diagnostic ultrasound: the role of American radiologists. Am J Roentgenol 1993;**160**:189–194.

[66] Gramiak R, Shah PM. Echocardiography of the aortic root. Invest Radiol 1968;**3**:356–366.

[67] Gramiak R, Shah PM, Kramer DH. Ultrasound cardiography: contrast studies in anatomy and function. Radiology 1969;**92**:939–948.

[68] Stride E, Edirisinghe M. Novel microbubble preparation technologies. Soft Matter 2008;**4**:2350–2359.

[69] Dijkmans PA, Juffermans LJ, Musters RJ, van Wamel A, ten Cate FJ, van Gilst W, Visser CA, de Jong N, Kamp O. Microbubbles and ultrasound: from diagnosis to therapy. Eur J Echocardiogr 2004;**5**:245–256.

[70] Deshpande N, Willmann JK. Microparticle-and nanoparticle-based contrast-enhanced ultrasound imaging. In: Chen X, editor. *Nanoplatform-Based Molecular Imaging*. Hoboken (NJ): John Wiley & Sons; 2011. p 233.

[71] Feinstein SB, ten Cate FJ, Zwehl W, Ong K, Maurer G, Tei C, Shah PM, Meerbaum S, Corday E. Two-dimensional contrast echocardiography. I. In vitro development and quantitative analysis of echo contrast agents. J Am Coll Cardiol 1984;**3**:14–20.

[72] Feinstein SB. Contrast agents for ultrasonic imaging. US patent 4,718,433. 1988.

[73] Kim S. Liposomes as carriers of cancer chemotherapy. Drugs 1993;**46**:618–638.

[74] Mauk MR, Gamble RC, Baldeschwieler JD. Targeting of lipid vesicles: specificity of carbohydrate receptor analogues for leukocytes in mice. Proc Natl Acad Sci U S A 1980;**77**:4430–4434.

[75] Villanueva FS, Jankowski RJ, Klibanov S, Pina ML, Alber SM, Watkins SC, Brandenburger GH, Wagner WR. Microbubbles targeted to intercellular adhesion molecule-1 bind to activated coronary artery endothelial cells. Circulation 1998;**98**:1–5.

[76] Weissleder R, Bogdanov A, Neuwelt EA, Papisov M. Long-circulating iron oxides for MR imaging. Adv Drug Deliv Rev 1995;**16**:321–334.

[77] Davis FF. The origin of pegnology. Adv Drug Deliv Rev 2002;**54**:457–458.

[78] Gabizon A, Papahadjopoulos D. Liposome formulations with prolonged circulation time in blood and enhanced uptake by tumors. Proc Natl Acad Sci U S A 1988;**85**:6949–6953.

[79] Klibanov AL, Khaw BA, Nossiff N, O'Donnell SM, Huang L, Slinkin MA, Torchilin VP. Targeting of macromolecular carriers and liposomes by antibodies to myosin heavy chain. Am J Physiol 1991;**261**:60–65.

[80] Weissleder R, Mahmood U. Molecular imaging. Radiology 2001;**219**:316–333.